Response of the electron density profiles to geomagnetic disturbances in January 2005

RUMIANA BOJILOVA AND PLAMEN MUKHTAROV

Section of Ionospheric Physics, Department of Geophysics, National Institude of Geophysics, Geodesy and Geography, Acad. G. Bonchev Bl. 3, Sofia 1113, Bulgaria
(rbojilova@geophys.bas.bg)

Received: February 13, 2019; Revised: April 12, 2019; Accepted: May 22, 2019

ABSTRACT

The ionospheric response to geomagnetic storms is usually investigated by considering the variability of the critical frequency of the F2-layer (foF2) or the total electron content (TEC) because these two parameters are directly measured by the ionosonde stations and the Global Navigation Satellite Systems (GNSS). In the present paper, however, the reaction is explored by using the vertical profiles of the electron density, $N(h)$, reconstructed by manually scaled ionosonde measurements at the station Sofia (42.4°N, 23.2°E). The mid-latitude ionosheric response to three geomagnetic storms that occurred in January 2005 is presented as this period has been selected because no major sudden stratospheric warming occurred during this month, and the winter 2005 is given in the literature as an example of a "normal" year. Hence the observed ionospheric response to the considered geomagnetic storms can be attributed mainly to the external forcing. Besides the traditional parameters foF2 and TEC, a particular attention is paid to the variability of the peak electron density height (hmF2). This study reveals for the first time that the main contribution to the response of the midlatitude ionosphere to moderate/intense winter geomagnetic storms is associated with significant enhancements of short-period quasi-diurnal oscillations with period of 6–7 hours observed in both foF2 and hmF2. An explanation of the main mechanisms responsible for the distortion of the diurnal ionospheric variability during these storms is offered. This result is especially important for the ground-based HF radio communications.

Keywords: ionosphere response, geomagnetic disturbances, ionosonde, *TEC*

1. INTRODUCTION

The ionospheric day-to-day variability is usually caused by the following drivers; (i) solar variability with a time scale of several days; (ii) geomagnetic storms, and (iii) those forcing mechanisms that originate in the lower atmosphere but have impact on the ionosphere by different coupling processes (dynamic and electrodynamic, radiative, transport, chemistry of atmospheric constituents, etc.). The first two drivers are known as forcing from above or external forcing and the last one is accepted as a forcing from

Stud. Geophys. Geod., 63 (2019), 436–454, DOI: 10.1007/s11200-019-0510-6

below or internal one. While the geomagnetic storms are the most significant external driver the sudden stratospheric warmings (SSW) and particularly the major ones are usually the strongest internal driver. This means that when the response of the ionosphere to a geomagnetic storm in winter is considered the presence of a SSW event has to be taken in mind also.

Geomagnetic storms are excited through the interaction between coronal mass ejections (CMEs) and the Earth's magnetic field. They are accompanied by energy inputs leading to substantial effects into the upper atmosphere and the ionosphere. Usually during the geomagnetic disturbances the aurora particle precipitations and high-latitude ionospheric currents are significantly strengthened. As a result, the Joule heating, together with the increased high-latitude ionization and pervasion of electric fields to low latitudes have a significant impact on the "quiet-time" dynamics and structure of the thermosphere and ionosphere (*Trichtchenko et al., 2007*; *Astafyeva et al., 2015*).The global response of the ionosphere to these strong geomagnetic disturbances is well studied (*Prölss, 1980, 2008*; *Muhtarov and Kutiev, 1998;Rishbeth, 1998*; *Buonsanto, 1999*; *Fuller-Rowell et al., 2000*; *Kutiev and Muhtarov, 2001, 2003*; *Balan et al., 2010*).

It is well known that during geomagnetic storms the dynamics, electrodynamics and chemistry of the atmosphere-ionosphere system are modified on a global scale and cause positive and/or negative phases of ionospheric response. The occurrence of the positive/negative response depends mainly on the latitude/longitude, season and the storm onset and maximum (*Andonov et al., 2011*; *Mukhtarov et al., 2013*; *Mukhtarov and Bojilova, 2017*). Three dominant causes of storm effects have been suggested to explain these phases of ionospheric storms: thermospheric composition changes, neutral wind perturbations and the electric fields of magnetospheric origin (*Mendillo, 2006*). The negative phase of ionospheric storms is mainly due to the composition changes (*Prölss, 1980,2011*; *Rishbeth, 1991*), i.e. the thermosphere becomes richer in molecular nitrogen and poorer in atomic oxygen (the O/N_2 ratio decreases). *Wang et al., (2010)* demonstrated the relationship between the change of the O/N_2 ratio and the negative reaction during the storm. Their study has presented clear evidence that the negative storm response observed in the total electron content (*TEC*) maps at high- and mid-latitudes is directly related to the changes in the O/N_2 ratio.

Recently the reasons leading to a positive phase of the ionospheric storms have been intensively studied. Observations and numerical simulations revealed that the combined effects of the disturbed thermospheric wind and electric fields are the main drivers (*Lin et al., 2005*; *Lu et al., 2008*; *Balan et al., 2010*). *Kelley et al. (2004)* suggested that a strong eastward prompt penetration electric field (PPEF) in the presence of daytime production of ionization can strengthen the equatorial plasma fountain to a super plasma fountain, which, in turn, can lead to positive ionospheric storms at midlatitudes. It is also known that the global thermospheric disturbances caused by the auroral heating produce long duration electric fields, known as disturbance dynamo electric fields (DDEF) (*Blanc and Richmond*, *1980*). They dominate the low latitudes with a delay of 4–5 h from the first incidence of the PPEF following the storm onset. These are long-lasting electric fields and have polarity that is nearly opposite to that of the PPEF (*Richmond et al., 2003*). The positive ionospheric storms observed at subauroral latitudes have been attributed to the expansion of the convection electric fields at higher latitudes which can push plasma to

high altitudes where the recombination is much slower, i.e. plasma accumulation occurs (*Foster et al*., *2002*; *Heelis et al., 2009*). Further, the geomagnetically driven equatorward winds can additionally strengthen the positive storms at subauroral latitudes also (*Balan et al., 2010*).

It has been already mentioned that the geomagnetic storms dramatically change the ionosphere particularly the electron density and its vertical distribution, as well as the *TEC*. The appearance of such large-scale electron density disturbances affects all branches of telecommunication and navigation and can have significant, adverse effects on ground- and space-based technological systems (e.g. *Jakowski et al*., *2005*,*2008*; *Stankov and Jakowski*, *2007*). The negative ionospheric storms in which the electron density and *TEC* decrease much below their "quiet-time" levels causing serious problems in ground-based HF radio communications. The positive ionospheric storms in which electron density and *TEC* increase much above their "quiet-time" levels can cause serious problems in satellite communication and navigation (such as time delay, range error and scintillations). Because the GPS signals are used by wide range of applications, any geomagnetic storm event which makes GPS signal unreliable could have significant impact on the society. Hence the monitoring of ionosphere as well as the detailed investigations of its response to forcing from above and below is among the important tasks of the ionosphere studies.

The basic aim of the present paper is to study in detail the ionospheric response over a mid-latitude ionosonde station Sofia to three geomagnetic storms that occurred in January 2005. The ionospheric response is examined by using the $N(h)$ profiles, i.e. the reaction of the entire ionosphere, from its bottom to the electron density maximum of the F-region, is traced out. Particular attention is paid to investigating the variability of the basic ionosphere parameters: critical frequency of the F2-layer, *fo*F2; altitude of the maximum electron density of the F2-layer, *hm*F2, and *TEC*. It is worth noting that the period January 2005 has not been accidentally selected. First, no major SSW occurred during this month and second, the mean solar activity seen in the solar Radio Flux *F*10.7 is around 99 (*Sahai et al*., *2011*), i.e. tending toward low solar activity. As a consequence of this the winter 2005 is given in some papers as an example of a background reference case corresponding to a "normal" year (*Manney et al.*, *2009*; *Winick et al.*, *2009*).

2. DATA AND METHOD FOR RECONSTRUCTING ELECTRON DENSITY PROFILES

The values for the planetary index of geomagnetic activity *Kp*, the disturbance storm time index (*Dst*) and the parameters of the solar wind are downloaded from *https://omniweb.gsfc.nasa.gov/*. The *TEC* values are provided by the Center for Orbit Determination of Europe (CODE) at Astronomical and Physical Institutes of the University of Bern (*ftp://ftp.unibe.ch/aiub/CODE/*). Because the *TEC* data have a grid spacing of 5° × 2.5° in longitude and latitude the nearest point to Sofia with coordinates (42.5°N, 25°E) was selected. The data for the critical frequency of the ionospheric F-region (*fo*F2) are obtained from the ionosonde station Sofia - SQ143 (42.4°N, 23.2°E). The KOS89 ionosonde is a ionosonde which does not produce automatically electron density profiles, $N(h)$ from the ionogram traces. It is important to note that this approach

is different from the method of true height conversion of ionograms used in the digital station for vertical incidence sounding from the Digisonde series of stations. On the basis of this method software is implemented for scaling the ionograms and deriving $N(h)$ profiles up to the maximum of the F-region (*Mukhtarov et al., 2013*).

The method used for deriving electron density profiles from scaled ionograms is described in detail by *Mukhtarov et al. (2013)*. It is based on the dependence of the virtual height of reflection on the radio-frequency and the refraction coefficient of the ionosphere. The dependence of the electron concentration on the height $N(h)$ (1/cm^3), expressed in plasma frequency f_N, is obtained by solving an integral equation.

The method for deriving $N(h)$ profiles from the ionogram traces is based on the known dependence of the virtual height h' of reflection on the radio-frequency f and the coefficient of refraction of the ionosphere n:

$$h'(f) = z_0 + \int_{z_0}^{z_{ref}} \frac{\partial f_N}{\partial f}\, dz\,, \tag{1}$$

$$n^2 = 1 - v\left\{1 - \frac{u_T}{2(1-v)} + \sqrt{u_L + \left[\frac{u_T}{2(1-v)}\right]^2}\right\}^{-1}, \tag{2}$$

where

$$v = \frac{f_N^2}{f^2}\,, \quad u_L = \frac{F_{H_0}}{f^2}\cos^2\alpha\,, \quad u_T = \frac{F_{H_0}}{f^2}\sin^2\alpha\,,$$

and $f_N = \sqrt{N/1.24\times10^4}$ is the plasma frequency. The angle between the group velocity of the radio wave and the geomagnetic field is denoted as α. According to the total vector of the geomagnetic filed and the inclination of the geomagnetic observatory Panagyurishte, the angle α for the territory of Bulgaria is 152° and the cyclotron frequency f_{H_0} is 1.313 MHz.

It is important to note the following two main features of the above mentioned method: (i) it is created particularly for the KOS89 ionosonde which defines well only the ordinary radio-frequency mode of reflection, and (ii) it is different from the method of true height conversion of ionograms used in the digital station for vertical incidence sounding from the Digisonde series of stations (*Reinisch and Huang, 1983*). Interactive software is developed for calculating the $N(h)$ profiles from the ionogram traces. In this way all available 15-minute ionograms have been processed for deriving the $N(h)$ profiles.

The response of the ionosphere to the geomagnetic storm is represented by the relative deviation of the used ionospheric parameter from its monthly median value (*Kutiev and Muhtarov, 2001*) and can be defined as:

$$V_{rel}\left(t\right)=\frac{V\left(t\right)-V_{med}\left(UT\right)}{V_{med}\left(UT\right)},$$

where $V\left(t\right)$ is observed *fo*F2, *hm*F2 or *TEC* at a given moment *t*, while $V_{med}\left(UT\right)$ represents a monthly median value at a given hour (in UT). In this way, the diurnal, seasonal and longtime solar dependence of ionospheric characteristics are filtered out (*Mukhtarov et al, 2017*).

3. RESULTS

Three moderate to intensive geomagnetic storms are observed in the selected period of January 2005. They can be clearly distinguished in the basic indexes showing the general conditions in both solar and geomagnetic activities during the considered month. The top panel of Fig. 1 presents daily values of solar radio flux from the whole solar disk with frequency 2800 MHz (10.7 cm) marked as *F*10.7. The considered period is characterized by quite large changes of the solar activity. While *F*10.7 has values around 85 s.f.u. (solar flux units) in the beginning and end of the month, it exceeds 140 s.f.u. values in the middle of the month. The middle plot of Fig. 1 shows planetary *Kp* index, giving information for the global variations of Earth's magnetic field, while the *Dst* index, which is a measure of the variability of the equatorial ring current, is displayed in Fig. 1 (bottom). The latter index indicates clearly the onset, the main and recovery phases of the geomagnetic storms as well as their magnitudes.

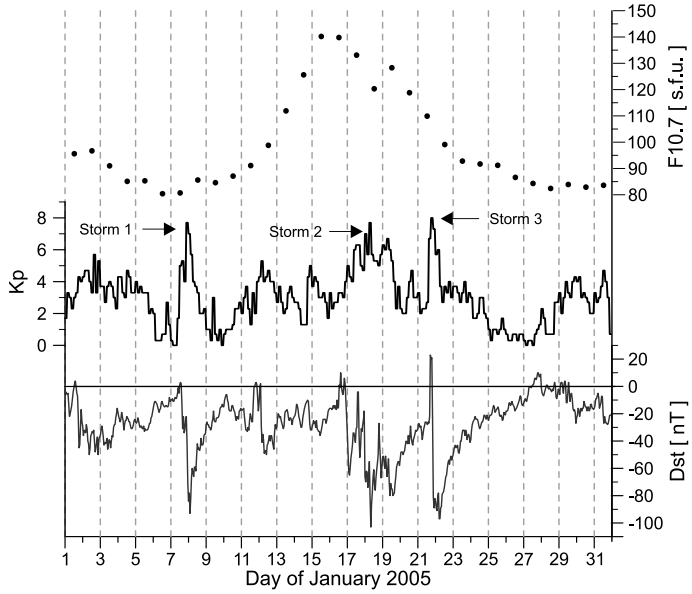

Fig. 1. Time variations in solar radio flux *F*10.7 (top), geomagnetic activity *Kp* index (middle), and the disturbance storm time *Dst* index (bottom).

Three distinct storms, with maximum $Kp > 7$, occurred in January 2005. The first storm begins on 7 January and the *Kp* index reaches to ~7.5–8 in the interval between 21–23 UT. It belongs to the so-called storms with a sudden storm commencement (SSC) seen in the *Dst*-index plot. The rapid increase of the *Kp* index is accompanied by a negative phase of the *Dst* index that reaches about –90 nT immediately after midnight on 8 January. As it has been already mentioned this storm occurs at low solar activity ($F10.7 \sim 85$ s.f.u.). According to its duration (around 18 hours) this storm is short-term one. The second storm, that is without a SSC, begins on 17 January and has a duration of several days. This storm is peculiar not only because the *Kp* index has values larger than 5 for more than 2 days and the *Dst* index has several negative minima corresponding to the rises of the *Kp* index but also because it occurs during higher solar activity ($F10.7 \sim 140$ s.f.u.). The *Dst* index has the largest negative reaction of about –105 nT on January 18, when the highest *Kp* index value is observed (close to 8). The recovery phase of the storm begins in the next day but is interrupted because of a new geomagnetic disturbance on January 21. The last geomagnetic storm considered is a short one, with duration of less than a day, and an interesting behavior of the *Dst* index. The sharp rise of the *Kp* index to values above 8 is accompanied by a sharp positive response in the *Dst* index, reaching values of ~20 nT in the afternoon and evening hours on 21 January. The subsequent *Dst*-index negative reaction reaches values close to –100 nT after midnight on 22 January and later the recovery phase is observed. Similarly to the first geomagnetic storm this one occurs also at low solar activity ($F10.7 \sim 95$ s.f.u.).

The undisturbed state of the ionosphere is usually described by the monthly median parameters. Fig. 2 presents the median values of *TEC* (Fig. 2a), *fo*F2 (Fig. 2b), *hm*F2 (Fig. 2c), and $N(h)$ profiles (Fig. 2d) for the month of January 2005. While the night values of *TEC* are about 6–7 TECU (1 TECU = 10^{16} electrons/m^2) and those of *fo*F2 are about 3 MHz, the corresponding daily values reach 15 TECU and 8 MHz respectively. The maximum height of F2 region is reached around midnight and is about 320 km, while in daytime it is between 220–240 km. These values should be taken into account because they are used as a basic condition to which the ionospheric response of the above mentioned parameters to the geomagnetic storms is determined. The median $N(h)$ profiles describe the undisturbed ionosphere up to the maximum of the F2 layer and will be compared with the disturbed ones during the storms. It is seen that the double-maximum distribution of the $N(h)$ is evident mainly around the maximum of the F2 layer and very rapidly decays with decreasing height.

3.1. Geomagnetic storm on 7–8 January 2005

The ionospheric response described by the relative values of *TEC*, *fo*F2 and *hm*F2, to the first storm is shown in Fig. 3. The upper plot of Fig. 3a displays the relative *TEC* during the period of 7–9 January. According to the *Kp*-index (Fig. 3c), the first disturbance occurred at 12 UT on 7 January when the *Kp* value rises to about 5. The *TEC* reaction is observed with a delay of several hours, around 17 UT, as the response is a positive one reaching values larger than 40%. At the storm maximum, around 23 UT, when the *Kp* index reaches values close to 8, there is no *TEC* response, but after

midnight on 8 January there is well-expressed negative response reaching to −50% (about 04 UT). The subsequent positive TEC response of 60% is observed at ~09 UT, occuring under relatively quiet geomagnetic conditions, i.e. $Kp \sim 4$. The relative values of *fo*F2 and *hm*F2 are presented in the Fig. 3a middle and bottom panels, respectively. It is evident that the variability of the relative *fo*F2 is similar to that of the relative *TEC*. This is an indication that in this case the changes in *fo*F2 to a large extent determine the changes in *TEC*. The maximum positive response of the relative *fo*F2 (~50%) occurs around 19 UT, when the value of geomagnetic activity $Kp \sim 4$. It is accompanied by a decrease in the relative *hm*F2 and a negative response close to −10% observed about 20 UT. The

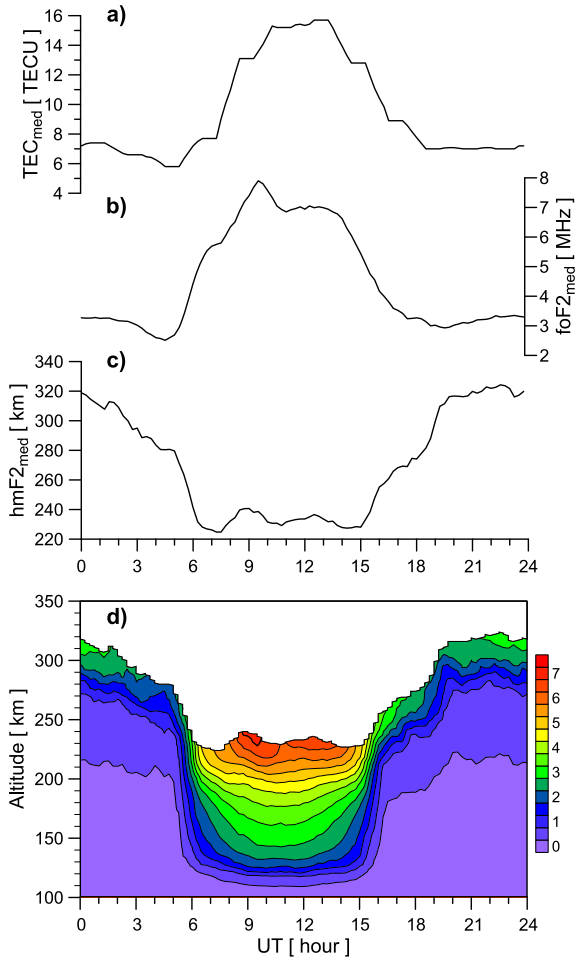

Fig. 2. Monthly median diurnal course of **a)** the total electron content TEC_{med}, **b)** the critical frequency (*fo*F2$_{med}$), **c)** the peak density height (*hm*F2$_{med}$), and **d)** vertical profiles of the electron density $N(h)_{med}$ up to the maximum of the F2 layer for January 2005.

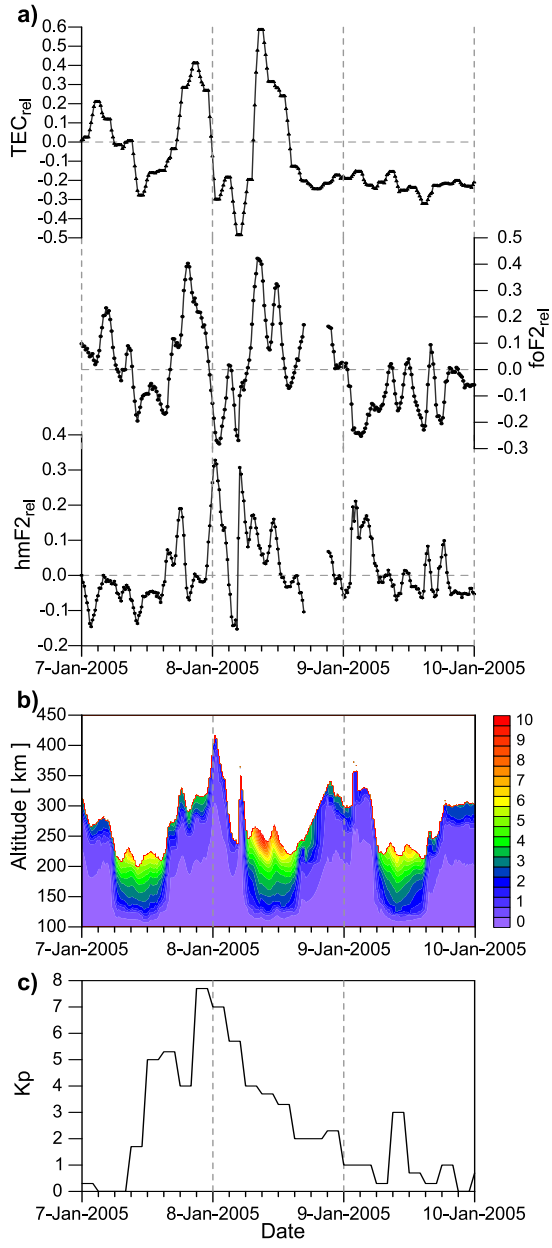

Fig. 3. **a)** Time variability of relative total electron content TEC_{rel} (top), relative critical frequency $foF2_{rel}$ (middle) and relative peak density height $hmF2_{rel}$ (bottom), **b)** profiles of the electron density $N(h)$ up to the maximum of F2 layer, and **c)** 3-hourly planetary index of geomagnetic activity *Kp* for the period of 7–9 January 2005.

positive(negative) response of the relative *fo*F2(*hm*F2) is due to the first sharp rise in the *Kp* index from 2 to 5 observed around 12 UT, i.e. it reveals a delay of several hours relative to the *Kp* index. The next negative(positive) response of the relative *fo*F2(*hm*F2) reaching values approximately –30(+30)% at around 01 and 05 UT on 8 January demonstrates again a delay to the maximum of the *Kp* index (as the relative *TEC*). On 8 January, during daytime, the relative *fo*F2 forms a well-expressed positive double peak at about 9 UT (~40%) and 12 UT (30%) when the *Kp* index is less than 4. The observed positive *fo*F2 response is a consequence of the geomagnetic disturbance during the evening and night hours of 7–8 January. The reaction of the relative *hm*F2 in daytime (between 6 and 15 UT) on 9 January is a positive one but not large as those of the relative *TEC* (~60%) and *fo*F2 (~40%); it is only about 15%. After that the ionosphere begins to restore its undisturbed state.

Figure 3b shows the $N(h)$ profiles, which describe the reaction of the entire, visible for the ground-based ionosonde, ionosphere, that extends from its bottom (~100 km) to the electron density maximum of the F2 layer, for the examined period of 7–9 January. Especially impressive are the large changes in the *hm*F2 after midnight on 8 January; first it rises to over 400 km around 01 UT, then falls sharply to almost 225 km (i.e. to the median height during daytime) at 04 UT and again immediately rises to ~350 km. These significant changes in the *hm*F2 are certainly caused by the disturbed dynamical regime due to the geomagnetic storm.

3.2. Geomagnetic storm on 17–19 January 2005

The ionospheric variability during the magnetic storms of 17–19 January 2005 was studied by *Shivalika et. al. (2013)*. The intense storm of 17 January started with SSC at 07:48 UT with vertical component of magnetic field B_z turning southward. At about 08:00 UT on 18 January maximum negative excursion of $Dst \sim -105$ nT (Fig. 1, bottom) is noted and the storm lasted until 19 January which was followed by the recovery phase on 20 January. It is worth noting that the response to this storm occurs under conditions of higher solar radiation ($F10.7 \sim 140$ s.f.u.). The ionospheric response of the second considered storm is shown in Fig. 4. Similarly to the first storm, here also Fig. 4a presents the relative *TEC* (upper panel), relative *fo*F2 (middle panel) and relative *hm*F2 (bottom panel) for the period of 17–20 January. The *Kp* index (Fig. 4c), shows that the first sharp increase (from 4 to 6) was observed between 08–09 UT on 17 January, i.e. almost together with the SSC of the storm. In the following hours, between 12 and 18 UT, the *Kp* index exceeds 6 and just before 18 UT it sharply drops below 5. It is important to note that all three above mentioned characteristics of the ionospheric response show a positive, almost synchronous, reaction that is almost without a delay. While the *TEC* response reaches about 90%, the *fo*F2 one is about 40% at ~15 UT and coincides with the maximum values of the relative *TEC*. As it has been mentioned above, the reaction of the relative *hm*F2 is almost synchronous with those of the other two parameters but reaches a maximum of 28% earlier, at ~09–10 UT. The next two maxima of the storm are respectively in the hours around 00–02 and 06–08 UT on 18 January, when the *Kp* index reaches values close to 7 in the first maximum and exceeds 7.5 in the second one. The well-expressed double-maximum response with 2–3 hours delay to the *Kp* index has been

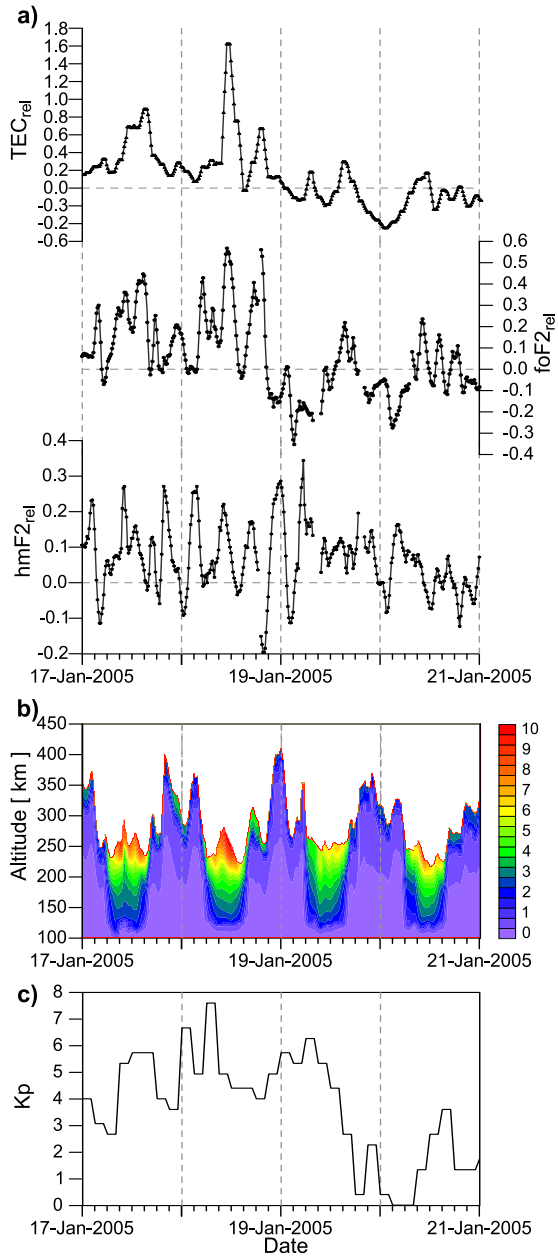

Fig. 4. The same as in Fig. 3, but for the period of 17–20 January 2005.

noted in both the relative *fo*F2 (40–55%) and *hm*F2 (20–25%), while the relative *TEC* reacted significantly positive only to the second *Kp* maximum with values exceeding 160% observed at ~12 UT.

The last increase of the *Kp* index, starting in the late hours on 18 January, is characterized again with two maxima around 00–02 and 06–08 UT on 19 January. It is accompanied with significant changes of the relative *hm*F2, varying between –20% in the night hours on 18 January and +35% observed at ~05–06 UT of the next day. The response of the relative *TEC* to this disturbance is significantly weaker than those of the previous *Kp* index increase. It ranges from negative after midnight (~ –15%) to positive (~15%) in the early morning hours (05–06 UT) on 19 January. The response of the relative *fo*F2 is predominantly negative and again almost synchronous with the *hm*F2 variations. It is worth noting that in all three considered relative quantities, *TEC*, *fo*F2 and *hm*F2, minima of –15%, –38%, –12%, respectively, are observed around 02 UT on 19 January, while at ~05–06 UT the three parameters have local maxima. The geomagnetic activity began to decrease in the hours after 09 UT on 19 January and after 15 UT on the same day it completely faded. Then the ionosphere gradually begins to recover. It is important to note that the large changes in the relative values of the three ionospheric characteristics are due to the fact that the storm of 17–19 January occurs under conditions of significantly higher solar activity ($F10.7 \sim 140$ s.f.u.) than the previous one (7–8 January), which is well evident in Fig. 1. The $N(h)$ profiles presented in Fig. 4b illustrate how the electron density changes with height during the period of 17–20 January. This geomagnetic storm, lasting more than 2 days, is characterized by synchronous oscillations of *fo*F2 and *hm*F2 with duration of several hours. As expected, the variability of *hm*F2 in the evening and night hours is significant, with the *hm*F2 varying on the average between 250 and 400 km. Similar *hm*F2 changes are observed also at midday hours, when *hm*F2 moved up to about 290 km on 17 and 18 January, i.e. well above the median daytime value of 230–240 km in January. The synchronous changes of *fo*F2 and *hm*F2 during the storm on 17–19 January are an indication for a strong impact of the disturbed dynamics not only on the height of the F2 layer but also on its electron concentration.

3.3. Geomagnetic storm on 21–22 January 2005

The third storm examined in the present study occurs in conditions of a not fully recovered ionosphere due to the geomagnetic storm on 17–19 January. An outstanding flare on 20 January 2005 was accompanied by a coronal mass ejection which arrived at the magnetopause at ~17:12 UT on 21 January producing a magnetic storm that reached minimum $Dst \approx -101$ nT at ~06:00 UT on 22 January, and its recovery phase endured until 27 January (*McKenna-Lawlor et. al., 2010*). Similarly to the first considered storm this one also develops in conditions of lower solar activity (~95 s.f.u.). The ionospheric response for the period of 21–23 January is presented in Fig. 5. This figure is analogous to Figs 3 and 4 which described the previous two storms. According to the *Kp* index (Fig. 5c) the geomagnetic storm begins at ~15 UT on 21 January, when it is rising sharply and reaches a maximum value of 8 in the hours between 18–20 UT. The response of the relative *TEC* (Fig. 5a, upper panel) is negative and occurs with some delay, as it reaches

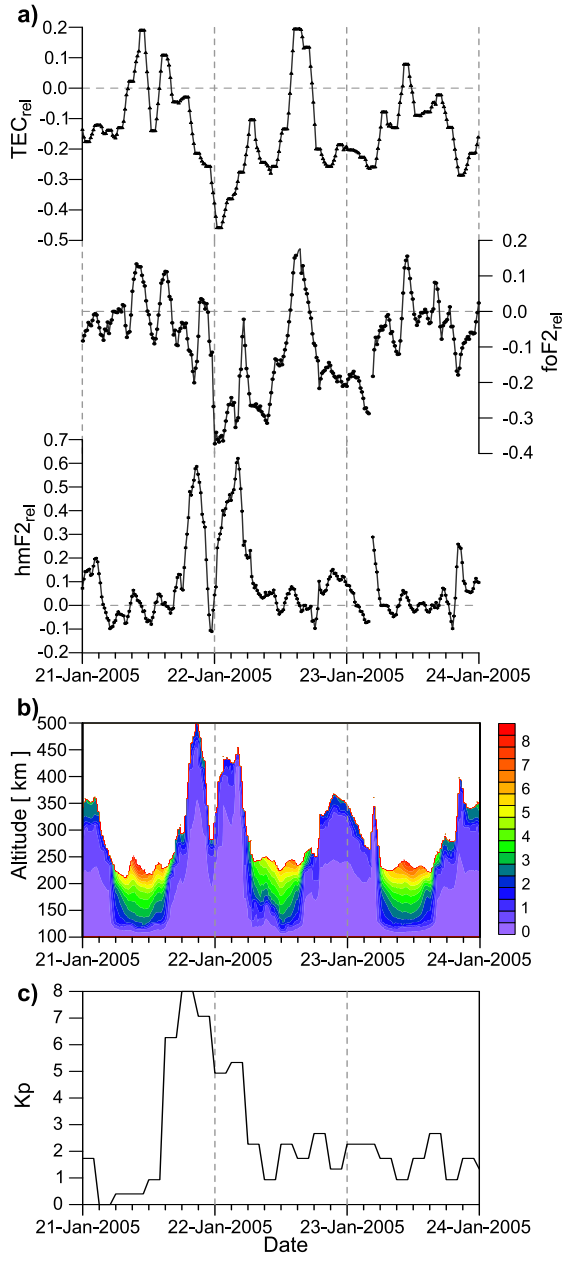

Fig. 5. The same as in Fig. 3, but for the period of 21–23 January 2005.

value of –46% in the hours between 00–02 UT on 22 January. The reaction of the relative *fo*F2 (Fig. 5a, middle panel) is also negative, especially after midnight on 22 January; its minimum, about –38%, coincides with that of the relative *TEC*, i.e. in the hours between 00–02 UT. The relative *hm*F2 response, in the hours around 18 UT on 21 January, is strongly positive and reaches 60% at 21 UT, when the *Kp* index is over 7. In the following hours, there was a sharp decrease in the relative *hm*F2 and a weak negative response (–12%) around midnight, followed by a new sharp rise and a positive response of the relative *hm*F2 (~62%) in the hours around 05 UT on 22 January. This, double-maximum variation of the relative *hm*F2 causes a synchronous change in the *fo*F2 response, while the *TEC* reacts only to the second disturbance of the *hm*F2. After 06 UT on 22 January, the *Kp* index has values not exceeding 4 but the relative *TEC* and *fo*F2 show a positive reaction, reaching up to 20%, during the period of 12–18 UT.

The altitude distribution of the electron concentration up to the F2 layer peak for the considered period of 21–23 January (Fig. 5b) very clearly demonstrates the double-maximum change in the *h*mF2. While the *hm*F2 reaches ~500 km at 21 UT on 21 January then falls down sharply to nearly 260 km (i.e. below the median height at night time) around midnight and after that immediately rises sharply up to ~420 km around 04–05 UT on 22 January. Similarly to the second geomagnetic storm these significant two elevations of the *hm*F2, accompanied with some increase in the electron concentration and partly in the *TEC* (especially in the second elevation), are largely the result of the disturbed dynamic regime.

4. DISCUSSION AND CONCLUSIONS

In this paper we have presented the mid-latitude ionospheric response to three, moderate to intensive, geomagnetic storms occurred in January 2005. The response is examined by using the $N(h)$ profiles registered by manually scaled ionosonde measurements at station Sofia, i.e. the reaction of the ionosphere from its bottom at height of about 100 km to the electron density maximum of the F2 layer is considered. Particular attention is paid also to the variability of the basic ionosphere parameters: *fo*F2, *hm*F2, and *TEC* as the last one is provided by the CODE for the nearest point to Sofia. It has been already mentioned that the winter 2005 was given as an example of a background reference case corresponding to a "normal" year (*Manney et al.*, *2009*; *Winick et al.*, *2009*) because no major SSW occurred during January 2005 and the mean solar activity ($F10.7 \sim 99$ s.f.u.) tended toward low solar activity. Therefore, the observed ionospheric response to the considered geomagnetic storms could be attributed mainly to the external forcing.

The main difference between the disturbed $N(h)$ profiles as well as the considered ionospheric anomalies $foF2_{rel}$ and $hmF2_{rel}$ (Figs 3–5) with the median ones presented in Fig. 2 is the significant amplification of the short-period quasi-diurnal oscillations with period of 6–7 hours. This feature is particularly well evident for the second geomagnetic storm, 17–18 January (see Fig. 4), when the *Kp* index (*Dst* index as well, Fig. 1, bottom plot) revealed a few disturbances. Especially large are the oscillations in the $hmF2_{rel}$

during the evening(night) time when in the frame of a few hours the *hm*F2 changes with more than 200 km (see for example Fig. 5b). To understand well the reason for the observed enhancement of the short-period quasi-diurnal oscillations in the considered ionospheric response over a typical mid-latitude station we have to mention first the main factors defining the quiet diurnal behavior of the F2 layer described by *fo*F2 and *hm*F2 (see Fig. 2b,c).

It is well known that both parameters have well defined diurnal course in winter where usually the day-time *fo*F2 values are several times larger than the nigh-time ones (see Fig. 2) predominantly due to low values of the night-time *fo*F2. During the day *fo*F2 is defined mainly by the production, loss and transport (diffusion, neutral winds and dynamo plasma drifts) processes while during the nigh-time it is preserved by the neutral wind dominated transport processes and possible plasma flux from the protonosphere (*Hanson and Patterson*, *1964*; *Shimazaki*, *1964*; *Risbeth, 1967*). It is found that the electromagnetic dynamo drifts are weak at quiet geomagnetic conditions (*Khan et al., 1985*; *Pi et al., 1993*) hence this mechanism is not important for the median diurnal variability of the *fo*F2. Thermal expansion (leading to changes in the production and loss rates at fixed height) of the atmosphere at sunrise as well as the strongest poleward wind at around noon-time driving ionization down magnetic field lines to lower heights where recombination is greater can produce the observed respectively morning maximum and midday bite out (*Saryo et al.*, *1989*; *Lynn et al*., *2014*; *Katamzi et al*., *2016*) well seen in Fig. 2b. The *hm*F2 diurnal course is defined predominantly by the neutral winds (*Rishbeth*, *1972*; *Zhang et al*., *1999*). It is known that the meridional winds tend to blow toward the pole by the day and toward the equator at night. In this way they push the plasma down along the magnetic field lines during the day, i.e. they decrease *hm*F2, and just the opposite, push the plasma up during the night, i.e. increase in *hm*F2. The production and loss rate have also some impact on the *hm*F2 variability manifesting themselves mainly by the changes in neutral composition and temperatures.

The main drivers of the ionospheric response to geomagnetic storms over a typical midlatitude station are thought to be changes in the thermospheric wind system, neutral composition and temperature. The effects of electric fields and currents can also have some contribution but in general it is accepted that it is of secondary importance. It has been mentioned in the Introduction that a strong eastward PPEF (*Kelley et al., 2004*) in the presence of daytime production of ionization can strengthen the equatorial plasma fountain to a super plasma fountain, which, in turn, can lead to positive ionospheric storms at midlatitudes. Such positive ionospheric response during the day-time has been observed during the Halloween geomagnetic storm on 29–30 October 2003 and described in detail by *Pancheva at al. (2016).* The long-lasting disturbance dynamo electric fields (*Blanc and Richmond*, *1980*) have dominant effect at low latitudes but they influence midlatitudes as well. Their effect has a delay usually half of that for low latitudes, i.e. 2–3 hours from the storm onset. These electric fields produce downward vertical plasma drift during the day leading to some decrease of the electron density (*Richmond et al.*, *2003*).

The auroral heating during the geomagnetic storms can alter the mean global circulation of the thermosphere. Whereas for quiet conditions there is a general upwelling in the summer hemisphere flow toward the winter one at higher levels, and downwelling

in the winter hemisphere, the storm-time heating adds a polar upwelling and equatorward flow in both hemispheres. Especially large is this disturbed flow during the night when the electron density is significantly decreased; this can explain the large anomalies observed in the evening/night values of *hm*F2. During the winter the disturbed flow usually reverses the poleward one coming from the summer hemisphere and producing in this way two circulation cells. This process seriously affects mainly the vertical and meridional wind velocities. Further, the increased downwelling at midlatitudes moves the air into regions of increased pressure, and produces compressional heating, i.e. the neutral temperature at midlatitudes changes and affects loss and production rates. Another consequence of the appearance of the disturbed equatorward flow is that it is acted upon by the Coriolis force, and turns westward. This zonal, westward wind can continue to build up even after the storm turns off and become considerably larger than the meridional wind at midlatitudes.

The produced geomagnetically disturbed flow seriously changes the mean neutral winds which have dominant influence on the diurnal variation of the *hm*F2. The disturbed flow has another important implication particularly important for the variability of the electron density, i.e. *fo*F2. The increased equatorward (or decreased poleward) wind at middle latitudes push the ionosphere higher up along magnetic field lines, where the loss rate is lower. This can contribute to a positive ionospheric storm effect. During winter downwelling of the poleward wind from the summer hemisphere has the opposite effects: air with low concentrations of molecular species, i.e. reach of atomic oxygen, is carried downward. Therefore, this leads to a decrease of the loss rate and an increase of production rate. These two effects determine the large positive response in *fo*F2 seen on 7–8, 17–18 and 22 January 2005. It is worth noting that usually the molecular-rich air at high latitudes carried by the equatorward circulation cannot reach latitudes lower than 50°N as it has been found by *Mukhtarov and Pancheva (2012).* This is another reason explaining why the ionospheric response over Sofia in the winter is predominantly positive one.

All the above mentioned drivers lead to anomalies in the median diurnal course of the $N(h)$ profile as a whole and the considered ionospheric parameters in particular. We underline that usually the *TEC* anomalies are similar to those in *fo*F2 with only a few small positive or negative *fo*F2 reactions not well seen in *TEC* (as for example, the positive *fo*F2 response on 18 January between 3 and 6 UT, Fig. 4). In order to explore the impact of geomagnetic activity on the diurnal variability of the midlatitude ionosphere in winter we determine the spectral components of the *hm*F2 anomalies for January 2005. We choose this parameter because its diurnal course is defined mainly by neutral winds and named the neutral winds are mostly disturbed during the geomagnetic storms.

The top plot of Fig. 6 presents the wavelet spectrum calculated from the relative *hm*F2 values. It reveals significant amplification of the oscillations with periods of 6–7 hours observed during the considered three geomagnetic storms and at the beginning of 2–3 January, when the *Kp* index reaches values close to 6, but the *Dst* index is not disturbed (see Fig. 1). The middle plot of Fig. 6 shows the instantaneous amplitudes of the 7-hour oscillation; it is seen that the largest amplitudes are observed during the geomagnetic storms of 17–18 and 21–22 January, when the amplitudes reache values 0.15–0.16. To clarify the relationship between the variability of the *Kp* index and the relative $hmF2_{rel}$ we calculate the cross-correlation function between the two quantities. The bottom plot of

Fig. 6 demonstrates the normalized cross-correlation functions between the *Kp* index and the relative *hm*F2$_{rel}$ values and between the *Kp*-index and the amplitudes of the 7-hour oscillation. Two important conclusions follow from this comparison:

- The basic shape of the cross-correlation function between *Kp* index and *hm*F2$_{rel}$ is similar to that between *Kp* index and the amplitudes of the 7-h oscillation. This result indicates that the main contribution to the positive response of the *hm*F2$_{rel}$ to *Kp* index disturbances is the generation of the quasi-diurnal 6–7-h oscillations in the relative *hm*F2$_{rel}$. The presence of these oscillations is confirmed also by the second peak (with time lag ~8 hours) seen in the cross-correlation function between the *Kp* index and *hm*F2$_{rel}$.
- The positive response of the relative *hm*F2$_{rel}$ reveals an average delay of about two hours with respect to the *Kp* index. This is probably the time needed for the changes in the neutral winds to take effect at mid latitudes.

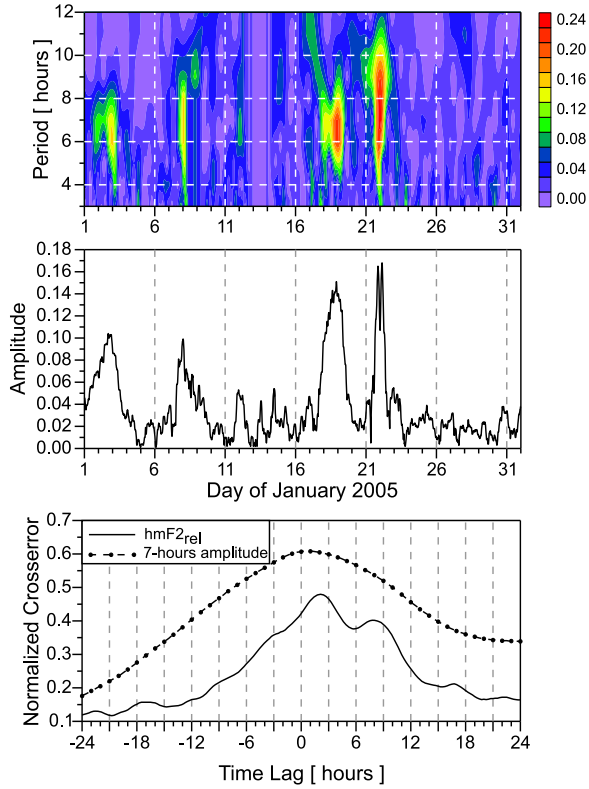

Fig. 6. **Top:** Wavelet spectrum calculated from the relative *hm*F2$_{rel}$ values, **middle:** amplitudes of the 7-hour oscillation, and **bottom:** normalized cross-correlation functions between the *Kp* index and the relative *hm*F2$_{rel}$ values, and between the *Kp* index and the 7-hour amplitudes calculated for January 2005.

The spectral and cross-correlation analyses have been applied only to the parameter $hmF2_{rel}$ however the almost synchronous in phase (out of phase) variations of $foF2_{rel}$ and $hmF2_{rel}$ well seen in Figs 4 and 5 (Fig. 3) indicate that the parameter $foF2_{rel}$ has also enhanced 6–7-h oscillations. When the variations between both parameters are in phase this means that the electron density response is defined mainly by the loss rate changes forced by the meridional winds while when they are out of phase the response is defined mainly by the production rate changes by downwelling of the poleward wind from the summer hemisphere that is reach of atomic oxygen.

In conclusion we note that for the first time the response of the midlatitude ionosphere to the moderate to intensive geomagnetic storms in winter is presented by significant enhancement of the short-period quasi-diurnal oscillations observed in the ionospheric parameters *fo*F2 and *hm*F2. An attempt has been made to clarify the main mechanisms responsible for disturbing the diurnal ionospheric variability during these storms.

References

Astafyeva E., Zakharenkova I. and Förster M., 2015. Ionospheric response to the 2015 St. Patrick's Day storm: A global multi-instrumental overview. *J. Geophys. Res.-Space Phys.*, **120**, 9023–9037, DOI: 10.1002/2015JA021629.

Andonov B., Mukhtarov P. and Pancheva D., 2011. Empirical model of the TEC response to the geomagnetic activity over the North American region. *Adv. Space Res.*, **48**, 1041–1048, DOI: 10.1016/j.asr.2011.05.007.

Balan N., Shiokawa K., Otsuka Y., Kikuchi T., Vijaya Lekshmi D., Kawamura S., Yamamoto M. and Bailey G.J., 2010. A physical mechanism of positive ionospheric storms at low latitudes and midlatitudes. *J. Geophys. Res.-Space Phys.*, **115**, A02304, DOI: 10.1029/2009JA014515.

Blanc M. and Richmond A.D., 1980. The ionospheric disturbance dynamo *J. Geophys. Res.*, **85(A4)**, 1669–1699.

Buonsanto M.J. 1999. Ionospheric storms: A review. *Space Sci. Rev.*, **88**, 563–601.

Foster J.C., Erickson P.J., Coster A.J., Goldstein J. and Rich F.J., 2002. Ionospheric signatures of plasmaspheric tails. *Geophys. Res. Lett.*, **29**, 1623, DOI: 10.1029/2002GL015067.

Fuller-Rowell T.J., Codrescu M.V. and Wilkinson M., 2000. Quantitative modelling of the ionospheric response to geomagnetic activity. *Ann. Geophys.*, **18**, 766–781.

Hanson W.B. and Patterson T.N.L., 1964. The maintenance of the nighttime F layer. *Planet. Space Sci.*, **12**, 979–997.

Heelis R.A., Sojka J.J., David M. and Schunk R.W., 2009. Storm time density enhancements in the mid latitude dayside ionosphere. *J. Geophys. Res.-Space Phys.*, **114**, A03315, DOI: 10.1029 /2008JA013690.

Jakowski N., Wilken V., Schlueter S., Stankov S.M. and Heise S., 2005. Ionospheric space weather effects monitored by simultaneous ground and spaced based GNSS signals. *J. Atmos. Sol.-Terr. Phys.*, **67**, 1074–1084.

Jakowski N., Mielich J., Borries C., Cander L., Krankowski A., Nava B. and Stankov S.M., 2008. Large scale ionospheric gradients over Europe observed in October 2003. *J. Atmos. Sol.-Terr. Phys.*, **70**, 1894–1903.

Katamzi Z.T., Habarulema J.B. and Giday N.M., 2016. Daytime twin-peak structures observed at southern African and European middle latitudes on 8-13 April 2012. *Ann. Geophys.*, **34**, 581–590, DOI: 10.5194/angeo-34-581-2016.

Kelley M.C., Vlasov M.N., Foster J.C. and Coster A.J., 2004. A quantitative explanation for the phenomenon known as storm-enhanced density. *Geophys. Res. Lett.*, **31**, L19809, DOI: 10.1029/2004GL020875.

Khan Z.M., Ara H., Iqbal S. and Nasir M., 1985. On the cause of fore-noon and post-noon bite-outs in foF2. *J. Atmos. Terr. Phys.*, **47**, 719–724.

Kutiev I. and Muhtarov P., 2001. Modeling of midlatitude F-region response to geomagnetic activity. *J. Geophys. Res.-Space Phys.*, **106**, 15501–15510.

Kutiev I. and Muhtarov P., 2003. Empirical modeling of global ionospheric foF2 response to geomagnetic activity. *J. Geophys. Res.-Space Phys.*, **108**, 1021, DOI: 10.1029/2001JA009134.

Lin C.H., Richmond A.D., Liu J.Y., Yeh H.C., Paxton L.J., Lu G., Tsai H.F. and Su S.-Y., 2005. Large-scale variations of the low-latitude ionosphere during the October–November 2003 superstorm: Observational results. *J. Geophys. Res.-Space Phys.*, **110**, A09S28, DOI: 10.1029/2004JA010900.

Lu G., Goncharenko L.P., Richmond A.D., Roble R.G. and Aponte N., 2008. A dayside ionospheric positive storm phase driven by neutral winds. *J. Geophys. Res.-Space Phys.*, **113**, A08304, DOI: 10.1029/2007JA012895.

Lynn K.J.W., Gardiner-Garden R.S. and Heitmann A., 2014. The spatial and temporal structure of twin peaks and midday bite out in foF2 (with associated height changes) n the Australian and South Pacific low midlatitude ionosphere. *J. Geophys. Res.-Space Phys.*, **119**, 10294–10304, DOI: 10.1002/2014JA020617.

McKenna-Lawlor S., Li L., Dandouras I., Brandt P.C., Zheng Y., Barabash S., Bucik R., Kudela K., Balaz J. and Strharsky I., 2010. Moderate geomagnetic storm (21–22 January 2005) triggered by an outstanding coronal mass ejection viewed via energetic neutral atoms. *J. Geophys. Res.-Space Phys.*, **115**, A08213, DOI: 10.1029/2009JA014663.

Manney G.L., Schwartz M.J., Krüger K., Santee M.L., Pawson S., Lee J.N., Daffer W.H., Fuller R.A. and Livesey N.J., 2009. Aura Microwave Limb Sounder observations of dynamics and transport during the record-breaking 2009 Arctic stratospheric major warming. *Geophys. Res. Lett.*, **36**, L12815, DOI: 10.1029/2009GL038586.

Mendillo M., 2006. Storms in the ionosphere: Patterns and processes for total electron content. *Rev. Geophys.*, **44**, RG4001, DOI: 10.1029/2005RG000193.

Muhtarov P. and Kutiev I., 1998. Empirical modeling of ionospheric storms at midlatitudes. *Adv. Space Res.*, **22**, 829–835.

Mukhtarov P., Penov N. and Pancheva, D. 2013. N(h) profiles derived from ionograms and their application for studying mid-latitude ionospheric response to geomagnetic storms. *C.R. Acad. Bulg. Sci.*, **66(9)**, 1315–1322.

Mukhtarov P. and Bojilova R., 2017. Influence of solar and geomagnetic activity on the ionosphere over Bulgaria. *C.R. Acad. Bulg. Sci.*, **70(9)**, 1289–1296.

Mukhtarov P. and Pancheva D., 2012. Thermosphere-ionosphere coupling in response to recurrent geomagnetic activity *J. Atmos. Sol.-Terr. Phys.*, **90–91**, **132–145**, DOI: 10.1016 /j.jastp.2012.02.013.

Pancheva D., Mukhtarov P. and Andonov B., 2016. Global structure of ionospheric TEC anomalies driven by geomagnetic storms. *J. Atmos. Sol.-Terr. Phys.*, **145**, 170–182, DOI: 10.1016 /j.jastp.2016.04.015.

Pi X., Mendillo M., Fox M.W. and Anderson D.N., 1993. Diurnal double maxima patterns in the F region ionosphere: substorm-related analysis aspects. *J. Geophys. Res.-Space Phys.*, **98**, 13677–13691.

Prölss G.W., 1980. Magnetic storm associated perturbations of the upper atmosphere: Recent results obtained with satellite-borne gas analyzers. *Rev. Geophys. Space Phys.*, **18**, 183–202.

Prölss G.W., 2008. Ionospheric storms at mid-latitudes: a short review. In: Kintner P.M. (Ed.), *Midlatitude Ionospheric Dynamics and Disturbances*. AGU Monograph **181**, American Geophysical Union, Washington, D.C., 9–24.

Prölss G.W., 2011. Density perturbations in the upper atmosphere caused by the dissipation of solar wind energy. *Surv. Geophys.*, **32**, 101–195.

Reinisch B. and Huang X., 1983. Automatic calculation of electron density profiles from digital ionograms: 3. Processing of bottomside ionograms. *Radio Sci*., **18**, 477–492.

Richmond A.D., Peymirat C. and Roble R.G., 2003. Long-lasting disturbances in the equatorial ionospheric electric field simulated with a coupled magnetosphere-ionosphere-thermosphere model. *J. Geophys. Res.-Space Phys*., **108**, 1118, DOI: 10.1029/2002JA009758.

Rishbeth H., 1967. The effect of winds on the ionospheric F2 peak. *J. Atmos. Terr. Phys*., **29**, 225–238.

Rishbeth H., 1972. Thermospheric winds and the F-region: A review. *J. Atmos. Terr. Phys.*, **34**, 1–47.

Rishbeth H., 1991. F-region storms and thermospheric dynamics. *J. Geomagn. Geoelectr.*, **43** (Suppl.), 513–524.

Rishbeth H., 1998. How the thermospheric circulation affects the ionospheric F2-layer. *J. Atmos. Terr. Phys.*, **60**, 1385–1402.

Sahai Y., Fagundes P.R., de Jesus R., de Abreu A.J., Crowley G., Kikuchi T., Huang C.S., Pillat V.G., Guarnieri F.L., Abalde J.R. and Bittencourt J.A., 2011. Studies of ionospheric F-region response in the Latin American sector during the geomagnetic storm of 21–22 January 2005. *Ann. Geophys*., **29**, 919–929, DOI: 10.5194/angeo-29-919-2011.

Saryo T., Takeda M., Araki T., Sato T., Tsuda T., Fukao S. and Kato S., 1989. A midday bite-out event of the F2-layer observed by MU radar. *J. Geomagn. Geoelectr*., **41**, 727–734.

Shimazaki T., 1964. Nighttime variations of F-region electron density profiles at Puerto Rico. *J. Geophys. Res.*, **69**, 2781–2797.

Stankov S.M. and Jakowski N., 2007. Ionospheric effects on GNSS reference network integrity. *J. Atmos. Sol.-Terr. Phys.*, **69**, 485–499.

Trichtchenko L., Zhukov A., Van Der Linden R., Stankov S.M., Jakowski N., Stanislawska I., Juchnikowski G., Wilkinson P., Patterson G. and Thomson A.W.P., 2007. November 2004 space weather events – real time observations and forecasts. *Space Weather*, **5**, S06001, DOI: 10.1029/2006SW000281.

Wang W., Lei J., Burns A.G., Solomon S.C., Wiltberger M., Xu J., Zhang Y., Paxton L. and Coster A., 2010. Ionospheric response to the initial phase of geomagnetic storms: Common features. *J. Geophys. Res.-Space Phys.*, **115**, A07321, DOI: 10.1029/2009JA014461.

Winick J.R., Wintersteiner P.P., Picard R.H., Esplin D., Mlynczak M.G., Russell III J.M. and Gordley L.L., 2009. OH layer characteristics during unusual boreal winters of 2004 and 2006, *J. Geophys. Res.-Space Phys.*, **114**, A02303, DOI: 10.1029/2008JA013688.

Zhang S.-R., Fukao S., Oliver W.L. and Otsuka Y., 1999. The height of the maximum ionospheric electron density over the MU radar. *J. Atmos. Sol.-Terr. Phys.*, **61**, 1367–1383.